Eur. Phys. J. D **22**, 99–107 (2003)
DOI: 10.1140/epjd/e2002-00232-x

THE EUROPEAN PHYSICAL JOURNAL D

On the structure of small lead clusters

J.P.K. Doye[a] and S.C. Hendy[2]

[1] University Chemical Laboratory[b], Lensfield Road, Cambridge CB2 1EW, UK
[2] Applied Mathematics, Industrial Research Limited, Lower Hutt, New Zealand

Received 17 July 2002
Published online 10 December 2002 –

Abstract. We have located putative global minima for all lead clusters with up to 160 atoms using a glue potential to model the interatomic interactions. The lowest-energy structures are not face-centred cubic, as suggested previously. Rather, for $N < 40$ the majority of structures are decahedral or hexagonal close-packed, and beyond this size the structures do not correspond to any of the structural forms commonly found in clusters. However, these latter clusters are not simply disordered. High symmetry, magic number clusters are still present, the most prominent of which is the 148-atom D_{3d} hexagonal barrel. We relate these structural preferences back to the form of the interactions.

PACS. 61.46.+w Nanoscale materials: clusters, nanoparticles, nanotubes, and nanocrystals – 36.40.Mr Spectroscopy and geometrical structure of clusters

1 Introduction

The structure of a cluster is one of its primary properties and one which has been intensely studied, experimentally and theoretically [1,2]. However, there is still much to be learnt about the fundamentals of cluster structure and the possible structures that can be formed. For atomic clusters with pair interactions, it is relatively well-understood how the form of the potential determines the observed structure. For example, the effects of the width of the potential well [3,4] and oscillations in the potential [5–7] have been systematically studied. However, for the systems that are of most interest, the interatomic interactions are usually much more complex. In particular, metal clusters, which are of great technological relevance [8], have a strong many-body character to their bonding.

This presents a number of challenges to our understanding of cluster structure in metals. First, there is the possibility that new types of structure could emerge as a result of many-body effects. Although, the structural types observed for pair potentials are also frequently observed for metals, *e.g.* the competition between icosahedral, decahedral and close-packed structures is also common for metals [9], there are an increasing number of intriguing exceptions. One seemingly common feature for small metal clusters is to exhibit structures with no discernible overall order [10–14]. However, it might be that the disorder is a result of new structural principles that cannot be fully satisfied at the sizes considered (hence the disorder), but which could lead to novel high symmetry structures at certain magic sizes [15]. Indeed, there are general grounds to expect high symmetry structures to emerge irrespective of the potential [16]. Studies that just reoptimize known cluster structures will of course miss such new features, and so it is important that efficient global optimization algorithms are used.

Secondly, the many-body character makes it increasingly difficult to relate the observed structure back to the interactions, even when the assumed form for the many-body potential is relatively simple. There has been some interesting progress recently in this area, namely into the causes of the disordered structures [17], and the effect of the range of the attraction and repulsion on the competition between icosahedral, decahedral and close-packed clusters [18], but there is much still to be discovered. This task is particularly important because of the difficulty in producing good empirical metal potentials (it is not feasible to study the sizes in which we are interested in any other way). One needs this kind of physical insight to understand the strengths and deficiencies of a potential and how it could be improved. It would also help one to discriminate between different potentials that purport to model the same material but give rise to different structures.

Lead clusters illustrate some of these challenges. The first theoretical study on large clusters by Lim *et al.* using a glue potential seemed to indicate that the most stable clusters at relatively small sizes (from at least $N \sim 55$) are face-centred cubic (fcc) [19], the preferred bulk structure [20]. This conclusion was based on a comparison of the energies of a series of Mackay icosahedra and fcc cuboctahedra. It is quite unusual to see bulk structures already being favoured at such small sizes, but this finding was rationalized on the basis of the particularly small

[a] e-mail: jpkd1@cam.ac.uk
[b] http://www-wales.ch.cam.ac.uk/~jon

value of γ, the ratio of the surface energies of the {100} and {111} faces [19]. Usually, the Mackay icosahedra have an energetic advantage at small sizes, because exclusively having {111} facets gives them an appreciably lower surface energy. Furthermore, these results were not inconsistent with the experiments in the literature at that time, which were mass spectroscopic studies on very small lead clusters [21,22], and electron diffraction experiments on very large clusters, which were identified as fcc, but with possibly some vestiges of amorphous structure [23].

This basic picture though has recently been challenged by both experimental [24] and theoretical [25] results. Electron diffraction of clusters from 3 to 7 nm indicates that the largest clusters are dominated by decahedra, but for the smaller clusters it was not possible to obtain an adequate fit to the diffraction pattern, suggesting that alternative structural models need to be considered [24].

Simulations of the melting and freezing of large lead clusters (modelled by the glue potential used by Lim *et al.* [19]) unexpectedly revealed that for a certain size range ($600 < N < 4\,000$, at least) fcc structures are not lowest in energy [25]. Instead, a new type of icosahedral structure, which is more stable than the fcc structures, spontaneously formed both on freezing and on heating at temperatures just below that for melting. Similar structures had been previously seen in some simulations of large lead clusters but it was not recognised that they could be lowest in energy [26]. They resemble anti-Mackay icosahedra [27], which have a Mackay icosahedral core but with most of the outer layer in "hexagonal close-packed" (hcp) surface sites rather than the "fcc" sites that would continue the packing in the Mackay icosahedra.

These results naturally raise intriguing questions about the structures of small lead clusters. What alternative structural models might be needed to understand the experimental results? Do lead clusters, as modelled by the glue potential, really favour fcc structures at small sizes? Lim *et al.* clearly showed that other standard forms were not lower in energy, so the structures would have to be somewhat unusual. Interestingly, a simple analysis using macroscopic properties as inputs suggested that lead would be a particular likely candidate for disordered clusters to be low in energy [17].

Here, we address some of these issues by performing global optimization for lead clusters with up to 160 atoms. We pay particular attention to characterizing the structures of these clusters and to understanding why the potential favours the lowest-energy structures.

2 Methods

To model the lead clusters we use a glue potential [28] of the form

$$E = \sum_{i<j} \phi\left(r_{ij}\right) + \sum_{i} U\left(n_i\right), \tag{1}$$

where $\phi(r)$ is a short-ranged pair potential, $U(n)$ is a many-body glue function and n_i is a "generalized coordination number" for atom i. n_i is defined as

$$n_i = \sum_{j} \rho\left(r_{ij}\right), \tag{2}$$

where $\rho(r)$ is an "atomic density" function. These three functions have been fitted for lead using a variety of bulk and surface properties [19]. The use of surface energies is particularly important for the application of this potential to model clusters. As well as clusters, this potential has been also used to model the surface reconstructions and pre-melting of low-index lead surfaces [29,30], and lead nanowires [31,32].

The choice of this empirical potential is motivated by the need for computational efficiency in order that global optimization is feasible for the sizes we consider here, and by our intention to compare with previous results. The use of *ab initio* electronic structure methods for lead is prohibitively expensive, especially as relativistic effects would need to be included to obtain reasonable results [20]. For example, sophisticated density functional calculations are unable to reproduce the experimental surface energies and anisotropies [33,34].

The functions $U(n)$, $\phi(r)$ and $\rho(r)$ are displayed in Figure 1. The pair potential has a very shallow well and so most of the binding energy comes from the glue term.

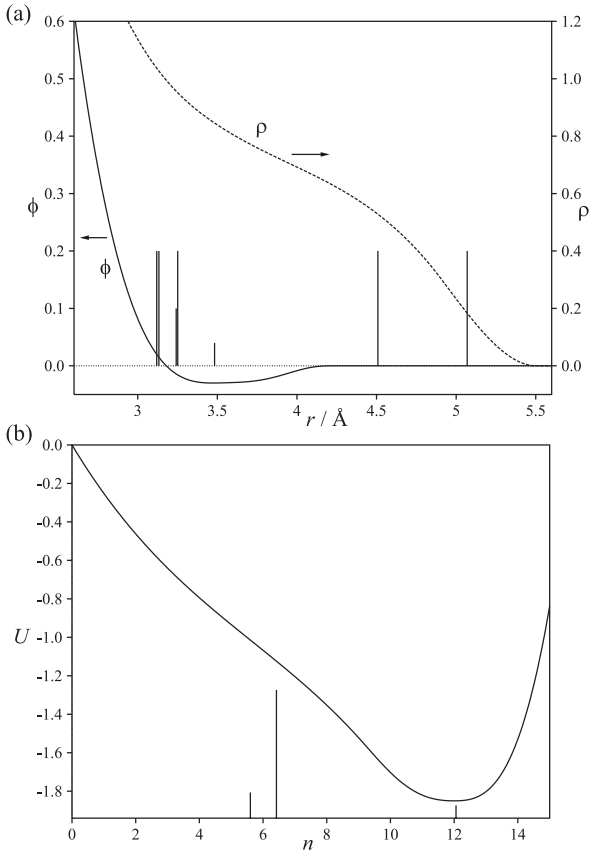

Fig. 1. The three functions that make up the lead glue potential: (a) $\phi(r)$, $\rho(r)$ and (b) $U(n)$. The pair distances and n_i values in the 13-atom decahedron are also plotted as impulses, with the heights proportional to the number that take that value.

The glue term has been chosen to have its minimum at $n = 12$, consistent with the designation of n as an effective coordination number. The form of $\rho(r)$ is particularly significant. As $\rho(r)$ decreases relatively slowly with increasing r beyond the minimum in the pair potential, next-nearest neighbours make a significant contribution to n. Therefore, the difference in surface energies between the {111} and {100} faces is small because, although an atom on a {100} face has fewer nearest neighbours, it has more next-nearest neighbours [19]. However, $\rho(r)$ then decreases relatively rapidly to zero at the cutoff at $r = 5.503$ Å, which typically occurs between the second and third neighbour shells.

For a pair potential the pair distances are the most important quantities. For example, the lowest-energy structure of a cluster involves a balance between maximization of the number of nearest neighbours, whilst minimizing the strain energy that results from nearest-neighbour pair distances deviating from the equilibrium pair value, $r_{\rm eq}$ [3]. However, for a glue potential, such as the current one, where the main contribution to the energy is from the glue function, the most important quantities are the n_i. Indeed, one of the key factors in generating a low-energy structure is to have the n_i values as close as possible to $n_{\rm eq}$, the value of n at the minimum of U. This can potentially lead to different ordering principles than for pair potentials. Only structures that have their nearest-neighbour pair distances close to $r_{\rm eq}$ are generally competitive for pair potentials. However, this constraint is relaxed for glue potentials, and particularly when, as in the current case, $\rho(r)$ initially falls off weakly with r.

For the atoms on the surface of a cluster $n_i < n_{\rm eq}$. Therefore, there will be a driving force for contraction of the surface to make the pair distances for the surface atoms smaller and hence their n_i larger. At equilibrium the surface contraction will be balanced by the increase in energy due to the resulting compression of the cluster core.

These considerations represent a particular problem for some of the usual forms for atomic clusters, such as the Mackay icosahedra and to a lesser extent decahedra. The inherent strain in these clusters results in pair distances between surface atoms that are longer than $r_{\rm eq}$, and so the compression needed to increase n_i for the surface atoms is particularly large. Therefore, these traditional structural forms are expected to become increasingly disfavoured by potentials for which the pair separation depends strongly on coordination number [17]. Instead, novel forms that are able to obtain large n_i values for the surface atoms, whilst not having too large an energetic penalty for compression of the cluster interior, could potentially be lowest in energy.

The global optimization of the lead clusters was performed using the basin-hopping [35,36] (or Monte Carlo minimization [37]) approach. This method has proved particularly successful in locating putative global minima for a wide variety of cluster systems [38]. The optimization task becomes rapidly more difficult with increasing N (*e.g.* the number of minima on the potential energy surface is thought to scale exponentially with N [39–41]) and so, of course, the possibility that we have not been able to obtain the true global minimum increases. However, the structural principles and trends are clear from our results.

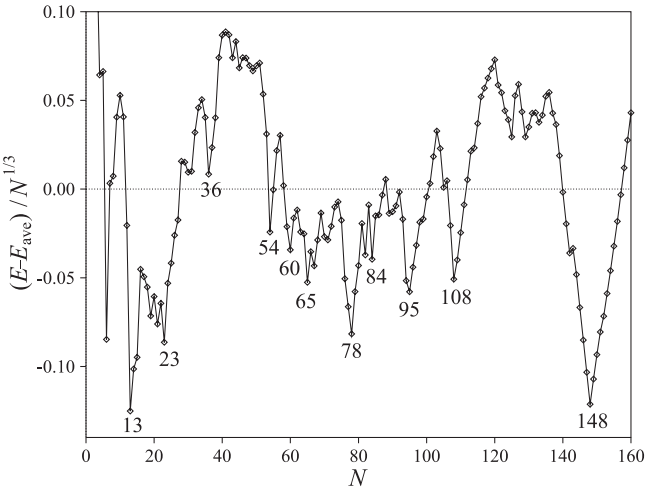

Fig. 2. Energies of the putative global minima relative to $E_{\rm ave}$, a four-parameter fit to these energies. $E_{\rm ave} = -2.0251N + 1.6608N^{2/3} + 1.3662N^{1/3} - 0.8634$.

3 Structures of the global minima

The energies and point groups for the putative global minima are given in Table 1. Point files will be made available online at the Cambridge Cluster Database [38]. The energies of the global minima are represented in Figure 2 in such a way that makes particularly stable clusters stand out. All clusters in the range $9 \leq N \leq 40$ are depicted in Figure 3 and a selection of particularly stable larger clusters in Figure 4.

First, we will look at the global minima for $N \leq 40$ in detail, before surveying more briefly the results for larger clusters. For $N \leq 8$ the clusters exhibit the same structures as typically seen for pair potentials. However, Pb_9 has a somewhat unusual form that can be described as two face-sharing octahedra, and so, as with Pb_{10}, is the beginning of an hcp cluster. Then for $N = 11$ and 12 more open structures with three-fold axes of symmetry are preferred.

Most of the global minima for $13 \leq N \leq 33$ are decahedral in origin. However, the growth sequence is not straightforward. The decahedra are generally asymmetric with the quasi-fivefold axis not passing through the centre of mass. So, although the growth sequence begins by adding atoms around the equator of the 13-atom Ino decahedron [42], before this shell is completed, asymmetric decahedra with a longer quasi-fivefold axis become lower in energy, starting at $N = 21$. Furthermore, sometimes part of the structure is distorted away from the ideal decahedral positions, *e.g.* at $N = 18$, 19, 26 and 32. There are also structures with two interpenetrating (Pb_{20}) and face-sharing (Pb_{24}) 13-atom decahedra, the latter with two additional shared capping atoms. It is noticeable that

Table 1. Energies and point groups (PG) of the putative global minima.

N	PG	Energy/eV	N	PG	Energy/eV	N	PG	Energy/eV	N	PG	Energy/eV
3	D_{3h}	–1.380851	43	C_s	–62.518056	83	C_1	–131.453946	123	C_2	–201.844885
4	T_d	–2.558548	44	C_s	–64.158589	84	D_2	–133.335862	124	C_2	–203.652142
5	D_{3h}	–3.711742	45	C_s	–65.887013	85	C_1	–134.977705	125	C_1	–205.483134
6	O_h	–5.214277	46	C_1	–67.545017	86	C_2	–136.725287	126	C_1	–207.149663
7	D_{5h}	–6.342793	47	C_1	–69.227454	87	C_1	–138.426910	127	C_1	–208.901679
8	C_{2v}	–7.665775	48	C_1	–70.926964	88	C_1	–140.139735	128	C_1	–210.764087
9	D_{3h}	–8.962242	49	C_2	–72.624639	89	C_{2v}	–141.978803	129	C_1	–212.620619
10	C_{2v}	–10.328111	50	C_1	–74.303601	90	C_s	–143.728686	130	C_1	–214.378335
11	C_{3v}	–11.771970	51	C_1	–75.989247	91	C_{2v}	–145.469445	131	C_1	–216.125616
12	D_{3h}	–13.351511	52	C_1	–77.748769	92	C_1	–147.190877	132	C_1	–217.911017
13	D_{5h}	–15.060197	53	C_1	–79.529727	93	C_1	–149.017327	133	C_1	–219.726303
14	C_{2v}	–16.488673	54	S_{10}	–81.438379	94	C_{2v}	–150.933479	134	C_1	–221.493988
15	C_{2v}	–17.971698	55	C_1	–83.050627	95	C_{2v}	–152.722173	135	C_1	–223.228659
16	C_{2v}	–19.359118	56	C_1	–84.670414	96	C_s	–154.419817	136	C_1	–225.006412
17	C_{3v}	–20.892141	57	C_1	–86.343451	97	C_1	–156.124859	137	C_1	–226.856548
18	C_1	–22.441282	58	C_1	–88.160853	98	C_1	–157.827739	138	C_2	–228.680493
19	C_{2v}	–24.029140	59	C_1	–89.961499	99	C_1	–159.582628	139	C_1	–230.562421
20	C_{2v}	–25.554526	60	C_1	–91.725507	100	C_1	–161.288978	140	C_1	–232.461447
21	C_{2v}	–27.160557	61	C_1	–93.369916	101	C_1	–163.018692	141	C_1	–234.347193
22	C_1	–28.700367	62	C_1	–95.068322	102	C_1	–164.713475	142	C_1	–236.226662
23	C_{2v}	–30.342369	63	C_1	–96.835577	103	C_1	–166.412388	143	C_1	–238.007461
24	D_{2h}	–31.834411	64	C_2	–98.559680	104	C_1	–168.225729	144	C_2	–239.879381
25	C_{2v}	–33.394629	65	C_2	–100.391525	105	C_1	–170.097176	145	C_s	–241.772812
26	C_s	–34.947504	66	S_4	–102.045664	106	C_1	–171.848423	146	C_2	–243.665845
27	C_{2v}	–36.526823	67	C_1	–103.803493	107	C_s	–173.738048	147	C_s	–245.558654
28	C_1	–38.036722	68	C_1	–105.470725	108	C_{2v}	–175.653403	148	D_{3d}	–247.451751
29	C_s	–39.653184	69	C_1	–107.136603	109	C_{2v}	–177.373836	149	C_1	–249.175286
30	C_s	–41.291166	70	C_1	–108.921031	110	C_s	–179.073251	150	C_s	–250.900806
31	C_{2v}	–42.914946	71	C_2	–110.659704	111	C_{2v}	–180.771206	151	C_1	–252.632151
32	C_{2v}	–44.475555	72	C_1	–112.360587	112	C_s	–182.477331	152	C_2	–254.384256
33	C_1	–46.064990	73	C_1	–114.048803	113	C_s	–184.174089	153	C_1	–256.115829
34	C_1	–47.687973	74	C_1	–115.771829	114	C_2	–185.939956	154	C_2	–257.846941
35	C_s	–49.363201	75	C_1	–117.552036	115	C_1	–187.649103	155	C_1	–259.573483
36	D_{3d}	–51.115236	76	C_2	–119.429639	116	C_1	–189.351898	156	C_2	–261.299215
37	C_{3v}	–52.716480	77	C_1	–121.236712	117	C_1	–191.105099	157	C_1	–263.019401
38	D_{3d}	–54.314542	78	C_2	–123.043586	118	C_1	–192.855140	158	C_2	–264.738883
39	C_1	–55.857448	79	C_2	–124.684422	119	C_1	–194.607282	159	C_1	–266.456122
40	C_2	–57.474215	80	C_1	–126.364903	120	C_1	–196.361528	160	C_1	–268.174733
41	C_s	–59.130894	81	C_1	–128.007123	121	C_1	–198.211397			
42	C_s	–60.803249	82	D_3	–129.829950	122	C_1	–200.012938			

the decahedral global minima generally have a significant proportion of surface atoms in {100}-type environments. This feature reflects the small energy difference between fcc {111} and {100} faces noted earlier. For materials that more strongly favour {111} faces, the most stable decahedral form is usually a Marks decahedron [43], because this structure maximizes the proportion of {111} faces, whilst retaining a relatively spherical shape. However, for lead the most stable decahedral clusters occur at $N = 13$ and 23 (Fig. 2).

The other set of ordered global minima found for $N \leq 40$ are the hcp clusters at $N = 35$–38. Again, these structures are somewhat unexpected, particularly as the fcc truncated octahedron is possible at $N = 38$, but this is further evidence of a preference for structures with a significant proportion of {100}-like faces.

Of the other global minima for $N \leq 40$, Pb_{17} is related to the 11-atom global minimum, but it is hard to discern any overall order for those at $N = 28$, 29 and 34. Pb_{39} and Pb_{40} are somewhat related to the preceding hcp structures, as is clear from the viewpoint chosen for

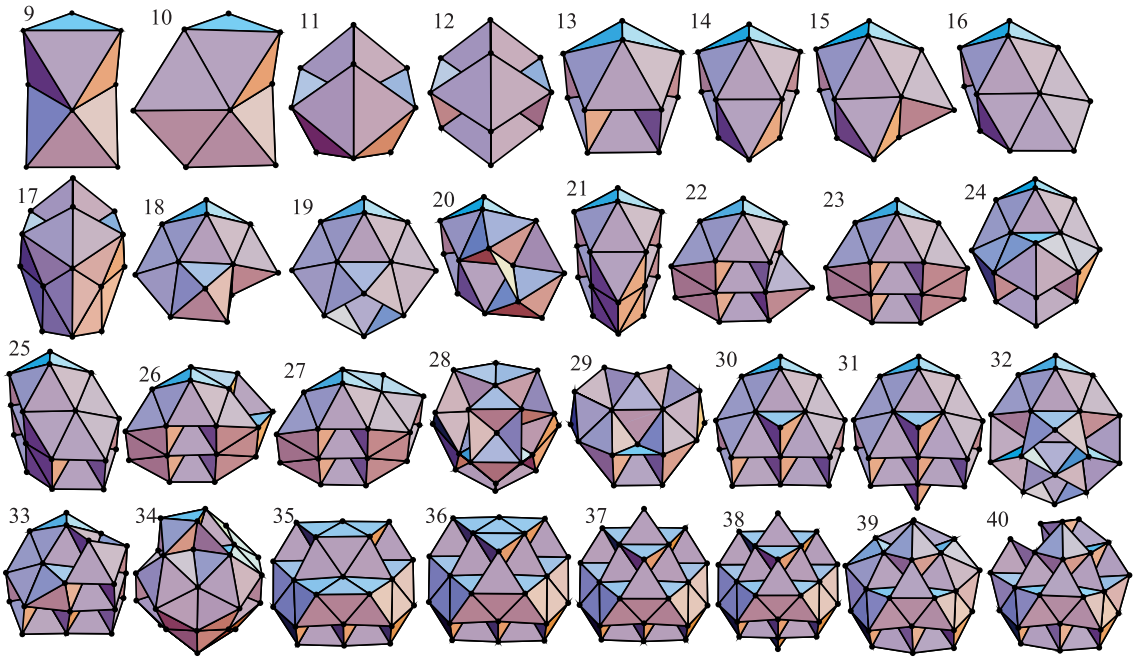

Fig. 3. The global minima for $N \leq 40$. Each cluster is labelled by the value of N.

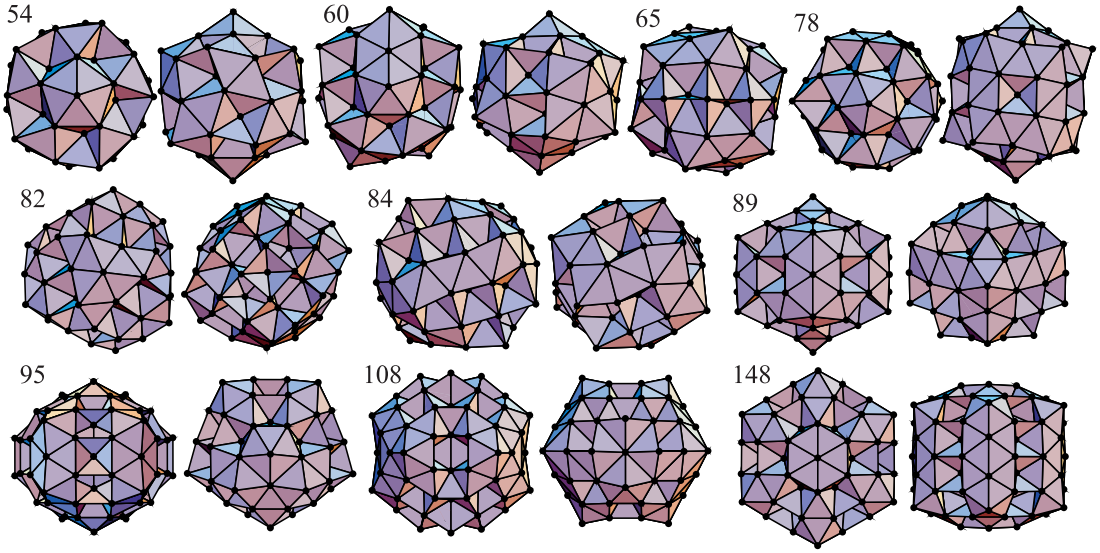

Fig. 4. A selection of particularly stable global minima for $N > 40$. Each cluster is labelled by the value of N. For most of the clusters two perpendicular views of the structure are given.

Figure 3, but again there is little order apparent on the other side of the cluster.

Beyond $N = 38$ none of the global minima that we have located can be assigned to any of the usual structural forms. However, it would be too simplistic just to characterize the clusters as disordered. From Table 1 we can see that high symmetry structures are still present. Furthermore, if the clusters were just disordered one would expect cluster properties to evolve fairly smoothly with size. However, it is clear from Figure 2 that there are "magic number" clusters that are particularly low in energy. Unsurprisingly, these magic numbers often correspond to the high symmetry clusters.

Although most of the clusters in this size range have no discernible *overall order*, there are common local surface motifs that are repeatedly visible. However, only at a relatively few sizes can these local preferences be assembled into a structure that has clear overall order.

As for the smaller clusters the surface structures of the global minima for $N > 40$ reflect the particularly low value of γ. However, this does not lead to structures with large {100} faces, but rather to many surface atoms with {100}-like environments. The surfaces are typically covered with a patchwork of squares and triangles. So on the flat regions of the surface it is common to see atoms surrounded by three triangles and two squares (there are two

Table 2. The contributions to the energy for a series of 55-atom structures, namely the global minimum (C_1), the fcc cuboctahedron (O_h), the Ino decahedron (D_{5h}) and the Mackay icosahedron (I_h). The structures are denoted by their point group (PG). $\langle E_i^{\rm bulk}\rangle$ and $\langle E_i^{\rm surf}\rangle$ are the average atomic energies for atoms in the interior of the cluster and on the surface, respectively. All the energies are measured in eV.

PG	Energy	$E_{\rm pair}$	$n_{\rm nn}$	$E_{\rm strain}$	$E_{\rm glue}$	$\langle n_i\rangle$	$\langle E_i^{\rm bulk}\rangle$	$\langle E_i^{\rm surf}\rangle$
C_1	–83.051	–1.796	216	4.684	–81.254	9.072	–1.885	–1.405
O_h	–82.559	–4.338	216	2.142	–78.220	8.783	–1.956	–1.360
D_{5h}	–82.438	–4.248	219	2.322	–78.190	8.800	–1.933	–1.365
I_h	–81.295	–5.944	234	1.076	–75.351	8.500	–1.946	–1.333

ways this can be achieved), rather than the six triangles or four squares, that are typical of {111} and {100} surfaces, respectively.

Pb_{54} is somewhat related to the Mackay icosahedron. It has a 12-atom uncentred icosahedron at its centre and a clear five-fold axis of symmetry. Along this axis it looks similar to the the D_{5h} structure that was found by Wolf and Landman as a low-energy isomer of the 55-atom Lennard-Jones clusters [44], and which is related to the icosahedron by a single rearrangement in which the structure is twisted around a five-fold axis. However, there is a canted arrangement of squares and triangles around the equator of the cluster.

The axial configuration of Pb_{54} seems to be quite a common motif, and similar patterns can be seen in one of the chosen views for $N = 60, 78, 95$ and 148, the last based on a six-fold rather than a five-fold symmetric version of the pattern, thus making the top surface flat, rather than pyramidal. As the size of these clusters increases the pattern is, of course, extended outwards. The resulting motif is clearest for the highly symmetric, 148-atom global minimum.

Pb_{148} is the most prominent magic number in this size range (Fig. 2). In shape, the cluster is a hexagonal barrel. Although the outer surface has a clear sixfold symmetry, this is in fact broken by the octahedron at the centre of the cluster.

4 Relationship between structure and potential

As flagged in the introduction, an important aim of this paper is not only to characterize the global minima for this lead potential, but to understand how the observed structures relate back to the form of the potential. We start by examining the decahedral 13-atom global minimum, for which the r_{ij} and n_i values have been included in Figure 1. It is noticeable that there is a significant dispersion of nearest-neighbour distances. In fact the longest distance is 11.7% longer than the shortest, which compares to a 2.3% difference for the same structure when optimized for the Lennard-Jones potential. As expected from the discussion in Section 2, the structure distorts to move the n_i values as close to $n_{\rm eq}$ as possible, rather than keeping the nearest-neighbour distances near to the minimum of the pair potential. This is achieved by an expansion along the fivefold axis and a contraction of the equator of the cluster. This reduces the n_i values for the two vertex atoms on the fivefold axis, but increases the n_i values for the other ten surface atoms, while maintaining the n_i value for the central atom close to $n_{\rm eq}$. A similar anisotropy of the pair distances has previously been noted by Lim *et al.* in their analysis of the lead cuboctahedra [19]; there is a greater contraction for the {100} faces of the cuboctahedra than the {111} faces because of the enhanced contribution to n_i from next neighbours across the diagonals of the squares on the {100} faces.

To understand why novel structural forms are observed for this lead potential, we take Pb_{55} as an example and compare the contributions to the energy from a series of competing structures (Tab. 2 and Fig. 5). The global minimum is based on the 54-atom structure illustrated in Figure 4 but with an additional surface atom. Also possible at this size are a fcc cuboctahedron, an Ino decahedron and a Mackay icosahedron.

In Table 2 we have decomposed the pair energy into two components:

$$E_{\rm pair} = -n_{\rm nn}\epsilon + E_{\rm strain}, \tag{3}$$

where $n_{\rm nn}$ is the number of nearest neighbours, ϵ is the depth of the pair potential, and $E_{\rm strain}$ is the energetic penalty for nearest-neighbour distances that deviate from $r_{\rm eq}$, the distance corresponding to the minimum of the pair potential. For this potential the contribution from next-nearest neighbours is zero, because of the position of the cutoff in the potential (Fig. 1a). More formally,

$$E_{\rm strain} = \sum_{i<j, r_{ij}<r_0} \epsilon - \phi(r_{ij}), \tag{4}$$

where r_0 is a distance criterion that distinguishes nearest from next-nearest neighbours. For all the structures we consider, there is a clear separation between these coordination shells.

As expected the pair energy only contributes a small fraction of the total energy. It is also noticeable that $E_{\rm strain}$ is of similar magnitude to $E_{\rm pair}$. This is in marked contrast to what occurs for pair potentials, where minimization of the strain energy is a key element of a structure's stability. $E_{\rm strain}$ for the global minimum is particularly large.

Although the pair energy is small in magnitude, it is structure sensitive and so it can still determine the relative stabilities of structures when the energies from the

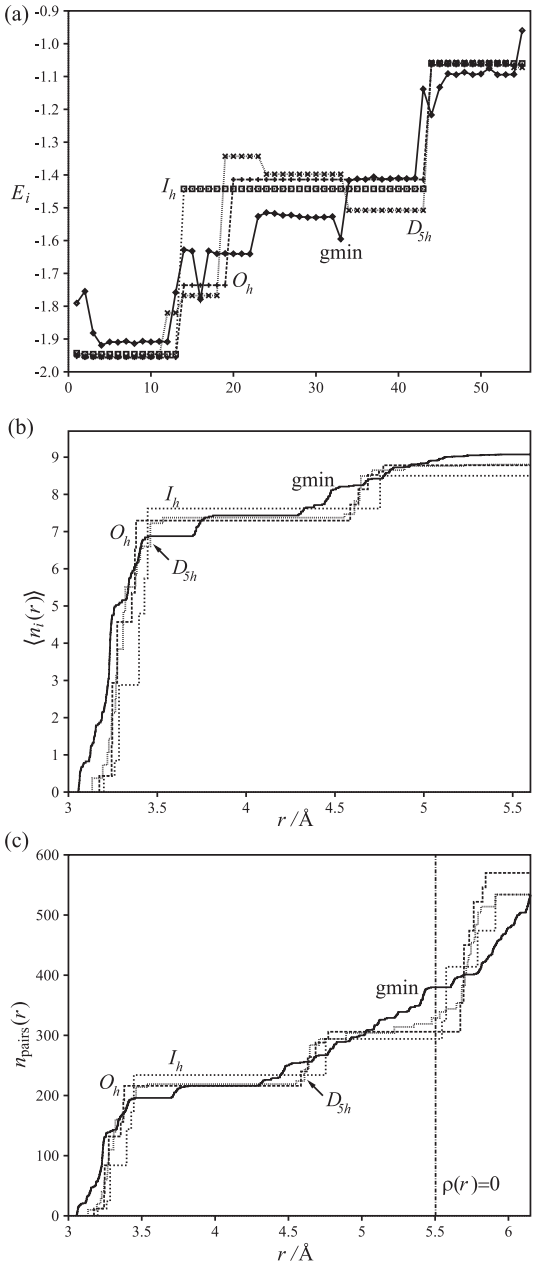

Fig. 5. A comparison of the properties of the 55-atom global minimum (gmin) to the fcc cuboctahedron (O_h), the Ino decahedron (D_{5h}) and the Mackay icosahedron (I_h), the same four clusters as in Table 2. (a) The atomic energies, E_i, for each atom in the cluster. The atoms have been ranked by their distance from the centre of mass, with atom 1 being the closest to the centre. (b) $\langle n_i(r_{ij} < r)\rangle$. (c) $n_{\rm pairs}(r)$.

glue term, $E_{\rm glue}$, are similar. For example, the major component of the difference in energy between the 55-atom cuboctahedron and decahedron is the greater pair energy of the cuboctahedron.

It is clear from Table 2 that the global minimum's stability is a result of its significantly lower glue energy, which is a result of the atoms being able to achieve n_i values that are closer to the ideal value, $n_{\rm eq}$. However, this lower glue energy is partially offset by the higher pair energy resulting from the distortion of the pair distances that is necessary to achieve an increase in n_i.

If we look at the atomic contributions to the energy (Tab. 2 and Fig. 5a) it is clear that the lower energy results from a lower average energy for the surface atoms (particularly atoms 13–33 in Fig. 5a), which outweighs the somewhat less favourable energies for the atoms in the interior of the cluster.

It is also interesting to understand what structural features of the global minimum lead to the larger value of $\langle n_i\rangle$. We analyse this in Figures 5b and 5c, first by looking at the cumulative contribution to $\langle n_i\rangle$ from pairs with distances less than r:

$$\langle n_i(r_{ij} < r)\rangle = \frac{1}{N} \sum_{i\neq j, r_{ij}<r} \rho(r_{ij}). \qquad (5)$$

It is particularly interesting to note that $\langle n_i^<(r)\rangle$ for the global minimum only becomes largest beyond 4.926 Å. Therefore, although the contribution to $\langle n_i\rangle$ from distances beyond this distance is small in magnitude, it is key in stabilizing the global minimum relative to the more conventional forms.

We can analyse this further by considering $n_{\rm pairs}(r)$, the number of pairs of atoms that are separated by less than r. It can be seen from Figure 5c that the number of pair distances within the radius of the cutoff distance for ρ is significantly larger for the global minimum than for the competing structures, which in turn correlates with the larger value of $\langle n_i\rangle$. However, this is only true because the cutoff is located between the second and third coordination shell. The cuboctahedron, decahedron and icosahedron all have a relatively narrow distribution of nearest-neighbour distances, which leads to a clear distinction between the second and third coordination shell. By contrast, the global minimum has a much more disperse nearest-neighbour shell and hence there is no clear distinction between a second and third neighbour shell. Instead, there is a steady increase in $n_{\rm pairs}(r)$ beyond the start of the second neighbour shell.

Although the above analysis has been presented for a single cluster, repeating this procedure for other sizes has confirmed the generality of the conclusions.

5 Conclusions

We have shown by locating the global minima for small lead clusters interacting with a many-body potential of the glue form that, contrary to the original conclusion of Lim *et al.*, these clusters do not adopt fcc geometries for $N \leq 160$. Instead, they form a series of novel structures that are a consequence of the many-body character of the potential. These results naturally lead one to wonder at what size bulk-like fcc structures will develop. To help us answer this question we have plotted in Figure 6 the energies of the global minima, alongside those for a number of sequences of high-symmetry structures and the novel

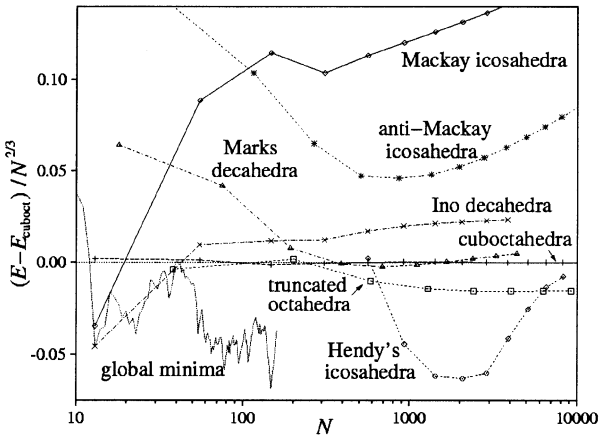

Fig. 6. A comparison of the energies of the global minima and the new icosahedra discovered by Hendy [25,45], to series of high-symmetric structures, which include Mackay and anti-Mackay icosahedra, cuboctahedra, truncated octahedra (with regular hexagonal {111} faces), Ino decahedra and Marks decahedra. The energies are measured with respect to $E_{\rm cuboct} = -2.0284N + 1.7929N^{2/3} + 0.9714N^{1/3} - 0.6342$.

icosahedral forms that Hendy obtained by simulations of freezing [25] and by construction [45].

The figure confirms that the icosahedra and decahedra are always higher in energy than the best fcc structures (except at the smaller sizes considered in the last section) and that the fcc truncated octahedra become slightly lower in energy than the cuboctahedra [19,25]. More interestingly, we can clearly see that both the global minima we have found and the new icosahedra produced by Hendy [25,45] are significantly lower in energy than the best fcc clusters. Thus, extrapolations between these two sizes ranges [46] suggest that fcc clusters might well not be the lowest in energy for intermediate sizes, and hence that fcc clusters are not lowest in energy until at least $N \sim 15\,000$ [45]. This is a surprising result, for although it is not uncommon to find small ($N < 100$) metal clusters that do not exhibit any of the usual cluster structures, it is unprecedented for this behaviour to persist up to such large sizes.

The results are also relevant to the ongoing issue of disordered metal clusters. Like recent theoretical results for gold [10–12], cadmium, zinc [14] and vanadium [13] many of our global minima do not fit with the fcc, hcp, decahedral and icosahedral structures that are often found for close-packed materials. However, to call these lead clusters disordered would be too strong because, although most of the clusters for $N > 40$ have no overall structural order, there are common local structural preferences which at a few sizes result in highly symmetric ordered structures that are particularly stable.

For pair potentials, clusters tend to retain a lattice structure away from the magic numbers, because it is unfavourable for the pair distances to deviate significantly from the equilibrium value. For example, most small Lennard-Jones clusters can be considered to be based upon Mackay icosahedra, either with an incomplete outer layer or covered by an ordered overlayer [47]. By contrast, for metal clusters the many-body character of the bonding can make it favourable to depart from or even abandon the lattice structure at sizes away from the magic numbers, because the atoms can then (in the language of the current potential) increase their effective coordination numbers (n_i's). A structure with no overall order results. Therefore, if one only examines a few cluster sizes the presence of particularly stable ordered structures may be missed.

From our analysis of the energetics of the competing structural forms we have seen that the shape of $\rho(r)$, in particular the shoulder and the position of the cutoff, is key to the stability of the novel structures that we find to be lowest in energy. This dependence on the cutoff is somewhat worrying both because it is a rather long-range feature of the potential and because its position is not physically motivated, but chosen more for computational convenience. These results illustrate how sensitively cluster structure depends on the potential; the correct determination of the relative energies of competing clusters is a stringent test of any potential [48].

Our results also help us to understand the structures exhibited by lead nanowires [32] modelled using the same potential. Gülseren *et al.* were surprised at the apparent contradiction between the non-fcc character of their nanowires and the cluster results of Lim *et al.* [19], and so suggested a number of reasons for the differing structural tendencies. However, our results show that the non-fcc character is common to both systems.

In this paper we have mainly focussed on the energies of the structures that we have considered. However, it should be remembered that differences in entropy can lead to changes in the equilibrium structure with temperature [48–51] and that the kinetics of structural development, be it through freezing [52–54] or growth [55–57], can significantly affect the cluster structure that results. Indeed, both of these effects may be required for a full understanding of experimental results.

J.P.K.D is grateful to the Royal Society for the award of a University Research Fellowship. S.C.H. would like to acknowledge the support of the ISAT linkages fund administered by the Royal Society of New Zealand.

References

1. R.L. Johnston, *Atomic and Molecular Clusters* (Taylor & Francis, London, 2002)
2. J.A. Alonso, Chem. Rev. **100**, 637 (2000)
3. J.P.K. Doye, D.J. Wales, R.S. Berry, J. Chem. Phys. **103**, 4234 (1995)
4. J.P.K. Doye, D.J. Wales, J. Chem. Soc., Faraday Trans. **93**, 4233 (1997)
5. J.P.K. Doye, D.J. Wales, S.I. Simdyankin, Faraday Discuss. **118**, 159 (2001)
6. J.P.K. Doye, D.J. Wales, Phys. Rev. Lett. **86**, 5719 (2001)
7. J.P.K. Doye, D.J. Wales, F.H. Zetterling, M. Dzugutov, J. Chem. Phys. (submitted), `cond-mat/0205374`

8. A.M. Argo, J.F. Odzak, F. Lai, B.C. Gates, Nature **415**, 623 (2002)
9. C.L. Cleveland, U. Landman, J. Chem. Phys. **94**, 7376 (1991)
10. I.L. Garzón, K. Michaelian, M.R. Beltrán, Phys. Rev. Lett. **81**, 1600 (1998)
11. K. Michaelian, N. Rendón, I.L. Garzón, Phys. Rev. B **60**, 2000 (1999)
12. I.L. Garzón, C. Rovira, K. Michaelian, M.R. Beltrán, P. Ordejón, J. Junquera, D. Sanchez-Portal, E. Artacho, J. Soler, Phys. Rev. Lett. **85**, 5250 (2000)
13. A. Taneda, T. Shimuzu, Y. Kawazoe, J. Phys. Cond. Matt. **13**, L305 (2001)
14. K. Michaelian, M.R. Beltrán, I.L. Garzón, Phys. Rev. B **65**, 041403(R) (2002)
15. J.M. Soler, I.L. Garzón, J.D. Joannopoulos, Solid State Commun. **117**, 621 (2001)
16. D.J. Wales, Chem. Phys. Lett. **285**, 330 (1998)
17. J.M. Soler, M.R. Beltrán, K. Michaelian, I.L. Garzón, P. Ordejón, D. Sánchez-Portal, E. Artacho, Phys. Rev. B **61**, 5771 (2000)
18. F. Baletto, R. Ferrando, A. Fortunelli, F. Montalenti, C. Mottet, J. Chem. Phys. **116**, 3856 (2002)
19. H.S. Lim, C.K. Ong, F. Ercolessi, Surf. Sci. **269/270**, 1109 (1992)
20. D.A. Young, *Phase diagrams of the elements* (University of California Press, Berkeley, 1991)
21. J. Mühlbach, P. Pfau, K. Sattler, E. Recknagel, Phys. Lett. A **87**, 415 (1982)
22. K. LaiHing, R.G. Wheeler, W.L. Wilson, M.A. Duncan, J. Chem. Phys. **87**, 3401 (1987)
23. A. Yokozeki, J. Chem. Phys. **68**, 3766 (1978)
24. M. Hyslop A. Wurl, S.A. Brown, B.D. Hall, R. Monot, Eur. Phys. J. D **16**, 233 (2001)
25. S.C. Hendy, B.D. Hall, Phys. Rev. B **64**, 085425 (2001)
26. H.S. Lim, C.K. Ong, F. Ercolessi, Comput. Mater. Sci. **2**, 495 (1994)
27. J.P.K. Doye, D.J. Wales, Z. Phys. D **40**, 466 (1997)
28. F. Ercolessi, M. Parrinello, E. Tosatti, Philos. Mag. A **58**, 213 (1988)
29. C.P. Toh, C.K. Ong, F. Ercolessi, Phys. Rev. B **50**, 17507 (1994)
30. A. Landa, P. Wynblatt, H. Häkkinen, R.N. Barnett, U. Landman, Phys. Rev. B **51**, 10972 (1995)
31. O. Gülseren, F. Ercolessi, E. Tosatti, Phys. Rev. B **51**, 7377 (1995)
32. O. Gülseren, F. Ercolessi, E. Tosatti, Phys. Rev. Lett. **80**, 3775 (1998)
33. L. Vitos, A.V. Ruban, H.L. Skriver, J. Kollár, Surf. Sci. **411**, 186 (1998)
34. P.J. Feibelmann, Phys. Rev. B **62**, 17020 (2000); **65**, 129902(E) (2002)
35. D.J. Wales, J.P.K. Doye, J. Phys. Chem. A **101**, 5111 (1997)
36. D.J. Wales, H.A. Scheraga, Science **285**, 1368 (1999)
37. Z. Li, H.A. Scheraga, Proc. Natl. Acad. Sci. USA **84**, 6611 (1987)
38. D.J. Wales, J.P.K. Doye, A. Dullweber, M.P. Hodges, F.Y. Naumkin, F. Calvo, J. Hernández-Rojas, T.F. Middleton, The Cambridge Cluster Database, `URL http://www-wales.ch.cam.ac.uk/CCD.html`
39. C.J. Tsai, K.D. Jordan, J. Phys. Chem. **97**, 11227 (1993)
40. F.H. Stillinger, Phys. Rev. E **59**, 48 (1999)
41. J.P.K. Doye, D.J. Wales, J. Chem. Phys. **116**, 3777 (2002)
42. S. Ino, J. Phys. Soc. Jpn **27**, 941 (1969)
43. L.D. Marks, Philos. Mag. A **49**, 81 (1984)
44. M.D. Wolf, U. Landman, J. Phys. Chem. A **102**, 6129 (1998)
45. S.C. Hendy, J.P.K. Doye, Phys. Rev. B **66**, in press (2002)
46. Although only one series of structures with the novel icosahedral form has been included in Figure 6, many are possible, which are characterized by the number of facets that are of a certain type [45]. If the energies of all these series were calculated, the size range over which these novel icosahedra are most stable would be significantly wider than suggested by Figure 6.
47. J.A. Northby, J. Chem. Phys. **87**, 6166 (1987)
48. J.P.K. Doye, D.J. Wales, J. Chem. Phys. **116**, 8307 (2002)
49. C.L. Cleveland, W.D. Luedtke, U. Landman, Phys. Rev. Lett. **81**, 2036 (1998)
50. J.P.K. Doye, M.A. Miller, D.J. Wales, J. Chem. Phys. **110**, 6896 (1999)
51. J.P.K. Doye, F. Calvo, Phys. Rev. Lett. **86**, 3570 (2001)
52. Y.G. Chushak, L.S. Bartell, J. Phys. Chem. B **105**, 11605 (2001)
53. F. Baletto, C. Mottet, R. Ferrando, Chem. Phys. Lett. **354**, 82 (2002)
54. H.-S. Nam, H.M. Hwang, B.D. Yu, J.-K. Yoon, `physics/0205024`
55. F. Baletto, C. Mottet, R. Ferrando, Phys. Rev. Lett. **84**, 5544 (2000)
56. F. Baletto, J.P.K. Doye, R. Ferrando, Phys. Rev. Lett. **88**, 075503 (2002)
57. F. Baletto, C. Mottet, R. Ferrando, Phys. Rev. B **63**, 155408 (2001)